Small-scale methane dispersion modelling for possible plume sources on the surface of Mars

K. S. Olsen,[1] E. Cloutis,[2] and K. Strong[1]

Received 4 July 2012; revised 4 September 2012; accepted 7 September 2012; published 11 October 2012.

[1] Intense interest in the characteristics of a methane source on Mars has been spurred by recent observations of a plume structure. The current NASA Mars Science Laboratory and future landers and orbiters will be tasked with understanding the sources of methane. The Canadian Space Agency's Mars Methane Analogue Mission, involving a simulated Mars micro-rover field campaign, was recently able to detect and measure the isotopic composition of methane seeping from boreholes in a serpentine mine in Québec. We aim to determine spatial limits for detecting such a point source above the terrestrial background concentration of methane using gradient transport models. We estimate the source strength to be on the order of $5.3 \times {}^{-10}$ kg s^{-1} and find that this produces detectable enhancements at distances less than 11.6 m from the source if there is no wind. These same models are applied to the Mars surface environment to determine whether an instrument on a rover would be capable of detecting a methane point source when not directly downwind of it. The estimated source strengths on Mars are much greater than at Jeffrey Mine and we find that these would be detectable at distances less than 30 m from the plume axis, which lies along the direction of advective transport. Much of the work done on modelling the Martian atmosphere uses large-scale general circulation models and this work examines the behaviour of methane plumes at very local scales.
Citation: Olsen, K. S., E. Cloutis, and K. Strong (2012), Small-scale methane dispersion modelling for possible plume sources on the surface of Mars, *Geophys. Res. Lett.*, *39*, L19201, doi:10.1029/2012GL052922.

1. Introduction

[2] The Mars Methane Analogue Mission (M3) deployed a micro-rover at the Jeffrey Mine, Québec, in June 2011 [*Cloutis et al.*, 2012], and deployed Carleton University's Kapvik rover at the Norbestos Mine, Québec, in June 2012. Both mines are located in the Ordovician Asbestos ophiolite [*Laurent and Hébert*, 1979; *Pinet and Tremblay*, 1995]. The background methane volume mixing ratio (VMR_{CH_4}) at Jeffrey Mine was measured to be 1.6 ppmv, with a standard deviation (σ_{SD}) of 0.5 ppmv, using a Picarro G1112-i cavity ring-down spectrometer. Separate measurements of methane emanating from a borehole in the mine wall found methane levels of 137.5 $\pm$ 0.3 ppmv and 200 $\pm$ 2 ppmv, while a measurement from a second borehole found 13.2 $\pm$ 0.2 ppmv. Measurements from near (<1 m) the boreholes showed a very rapid return to background methane mixing ratios. *In situ* measurements made by instruments on a rover, which may be unable to get sufficiently close to the methane source, would not be able to detect these enhancements, so the spatial range of detectable enhancement due to a source is of interest.

[3] The detection of methane on Mars [*Formisano et al.*, 2004; *Krasnopolsky et al.*, 2004; *Mumma et al.*, 2004] has been the subject of several recent atmospheric modelling studies. Observations from Earth by *Mumma et al.* [2009] showed a localized methane plume released over a short duration. While the results of this study have been questioned [*Zahnle et al.*, 2011; *Lefèvre and Forget*, 2009; *Mischna et al.*, 2011], subsequent studies of Mars from Earth and satellites also observed spatial and temporal variability in methane concentrations [*Fonti and Marzo*, 2010; *Geminale et al.*, 2011; *Krasnopolsky*, 2012].

[4] We use the observations presented by *Mumma et al.* [2009] and their subsequent examination by atmospheric models [*Mumma et al.*, 2009; *Lefèvre and Forget*, 2009; *Mischna et al.*, 2011] to estimate the strength of a local methane source. We locate it on the Martian surface at the landing site of NASA's Mars Science Laboratory (MSL), Gale Crater, and derive atmospheric parameters (temperature, pressure, mean wind velocity) from the Oxford-Laboratoire de Météorologie Dynamique-General Circulation Model (LMD-GCM) [*Forget et al.*, 1999], available at the website http://www-mars.lmd.jussieu.fr. We calculate a dispersion coefficient for methane in the Martian atmosphere at the surface and compute the VMR_{CH_4} distribution 1 m above the surface around the source using a gradient transport model [*Hanna et al.*, 1982]. We consider a variety of situations and examine the methane source observed at Jeffrey Mine for comparison.

2. Mars Surface Conditions

[5] The northwest corner of Gale Crater, 5.4°S and 137.8°E, is the chosen landing site of MSL. Its floor lies at an elevation of −4.4 km and can be considered smooth for convection purposes, allowing us to disregard effects from surface roughness. The LMD-GCM model resolution is too coarse (5° × 5°) to provide accurate simulations within the crater, but there are four grid points surrounding the crater rim that we can use to infer surface conditions inside the crater. We use climatological averages of pressure and temperature, with standard deviations, from midday (12:00) near the autumn equinox to avoid temperature highs and lows (solar longitude 180°–210°). Each of the four grid

[1]Department of Physics, University of Toronto, Toronto, Ontario, Canada.
[2]Department of Geography, University of Winnipeg, Winnipeg, Manitoba, Canada.

Corresponding author: K. S. Olsen, Department of Physics, University of Toronto, 60 St. George St., Toronto, ON M5S 1A7, Canada. (ksolsen@atmosp.physics.utoronto.ca)

0094-8276/12/2012GL052922

points are at different altitudes, determined from *Smith et al.* [1999], above and below a reference altitude, $z_\circ$. The model's climatological average surface pressures are used to determine $P_\circ$ at $z_\circ$ for each point, using the barometric law, $P(z) = P_\circ e^{(-z/H)}$, and a scale height of 11.1 km. The average from the four points was $P_\circ$ = 533 Pa, and the average of the model's climatological standard deviations was 17 Pa. Similarly, the temperature at $z_\circ$ was found to be 208 K, using an adiabatic lapse rate of −4.9 K/km [*Lindal et al.*, 1979]. Pressure at the crater floor is 792 ± 27 Pa, and the temperature at the crater floor is 229 K. The model's climatological standard deviations for temperature are small, ∼1 K, while the diurnal temperature variation on Mars can be around 60 K. The diffusion coefficient depends on temperature as $T^{3/2}$ and its accuracy is dominated by the temperature variation (equation (1) below). Temperature and pressure are used to determine the atmospheric number density: $n_\circ = A_\nu P/RT$, with Avogadro's number A_ν and the gas constant R. We estimate that in Gale Crater we have $n_\circ = 2.51 \times 10^{23}$ molecules m^{-3}, with a lower limit of 2.14×10^{23} molecules m^{-3} and an upper limit of 3.31×10^{23} molecules m^{-3} (for a temperature range of 259 to 179 K).

3. Gradient Transport Modelling

[6] The time evolution of the distribution of methane that has been injected into the atmosphere is governed by several factors: chemical interactions, diffusion, buoyancy, eddy motion and advection. We consider time scales significantly shorter than the lifetime of methane on Mars, estimated to be as much as several hundred years from photochemical analysis [*Wong et al.*, 2003] or on the order of hundreds of days to account for observations [*Lefèvre and Forget*, 2009; *Geminale et al.*, 2011], and assume that the contribution from chemical interactions is negligible. We also assume that the methane plume is at the same temperature as the ambient air and mixes sufficiently rapidly with CO_2 to result in no net buoyancy. In a situation with no wind, thermal motion will move methane molecules away from the source symmetrically. Winds will carry methane downwind from the source, where it will spread outward from its trajectory. Simple first-order methods are used for the model and to calculate the diffusion coefficient since there is large variability and uncertainty in several contributing factors, such as wind speed, pressure, temperature, and source strength.

[7] Interest in chemical diffusion on Mars has been largely devoted to high altitudes and high temperatures [*Catalfamo et al.*, 2009; *Rodrigo et al.*, 1990; *Izakov*, 1978]. Interest at the surface has been motivated by diffusion in soils and ice, and subsurface transport [*Hudson et al.*, 2007; *Hudson and Aharonson*, 2008; *Gough et al.*, 2010]. Diffusion is a thermal process governed by intermolecular collisions, and depends on pressure, temperature, particle size, and proximity. Chapman-Enskog theory [*Chapman and Cowling*, 1970] gives the coefficient of diffusion, D, for gas B in gas A as:

$$D = \frac{3}{8 n_\circ \sigma_{AB}^2} \sqrt{\frac{k_B T}{2\pi}\left(\frac{1}{m_A}+\frac{1}{m_B}\right)} \frac{f_D}{\Omega_{AB}} \quad (1)$$

where m_A and m_B are the molecular masses of the two gases in the mixture and k_B is Boltzmann's constant. σ_{AB} is the characteristic length of the mixture, determined by averaging the characteristic Lennard-Jones length of the two gases. f_D is a correction factor between 1.0 to 1.02, which we set to unity. Ω_{AB} is a dimensionless diffusion integral that depends on the characteristic Lennard-Jones energy ϵ and temperature. An analytic expression for Ω_{AB} is given in *Reid et al.* [1987] and values for ϵ and σ are tabulated in *Reid et al.* [1987] for air, CH_4, CO_2, N_2, Ar, and O_2. We are mixing CH_4 with Martian air (*Mair*), so we estimate ϵ_{Mair} and σ_{Mair} from assumed gas concentrations [*Owen et al.*, 1977]. Using ϵ_{Mair}/k_B = 190.1 K and ϵ_{CH_4}/k_B = 148.6 K, we find Ω_{Mair,CH_4} = 1.25 at 229 K, and using σ_{Mair} = 3.932 Å and σ_{CH_4} = 3.758 Å, we find σ_{Mair,CH_4} = 3.845 Å. We therefore calculate that the coefficient of diffusion for methane on the surface of Mars is 13.03 cm^2 s^{-1}. Variations in temperature produce a range of between 8.99 and 15.64 cm^2 s^{-1}. The diffusion coefficient of CH_4 in air on Earth is 0.2175 cm^2 s^{-1} [*Cowie and Watts*, 1971].

[8] Gradient transport models are solutions to the continuity equation [see *Hanna et al.*, 1982]:

$$\frac{\partial C}{\partial t} + u\frac{\partial C}{\partial x} + v\frac{\partial C}{\partial y} + w\frac{\partial C}{\partial z} = S + \frac{\partial}{x}K_x\frac{\partial C}{x} + \frac{\partial}{y}K_y\frac{\partial C}{y} + \frac{\partial}{z}K_z\frac{\partial C}{z} \quad (2)$$

where C is concentration; K_x, K_y, and K_z are radial diffusion coefficients; u, v, and w are wind speed in the x, y, and z directions; and S represents internal processes such as chemical reactions. In our models, we assume that $S \approx 0$ and diffusivity is constant in time and not dependent on direction, with $K_x = K_y = K_z = D$. The simplest case is for no wind, $u = v = w = 0$, which simplifies the equation to:

$$\frac{\partial C}{\partial t} = D\left(\frac{\partial^2 C}{\partial x^2} + \frac{\partial^2 C}{\partial y^2} + \frac{\partial^2 C}{\partial z^2}\right). \quad (3)$$

Solutions are given in *Hanna et al.* [1982] for a variety of initial conditions.

4. Estimation of Source Terms

[9] From *Mumma et al.* [2009], the total mass of methane released during a Mars plume event is 1.86×10^7 kg. *Mumma et al.* [2009] assumed that the emission is from a single source region and that the source strength must be 3.66 kg s^{-1} if active for 60 days (Q_{60}), 1.8 kg s^{-1} if active for 120 days (Q_{120}), or 0.63 kg s^{-1} if active for half a Mars year (Q_{344}). *Lefèvre and Forget* [2009] used the same release scenario, but with a much smaller mass, and performed their analysis with the LMD-GCM. They estimated the total mass of methane lost annually via photochemical processes, 2.6×10^5 kg, and released it from a single point over 60 days, resulting in a source strength of Q_{LF} = 0.050 kg s^{-1}. *Mischna et al.* [2011] used the Mars Weather Research and Forecasting (MarsWRF) GCM [*Richardson et al.*, 2007] to try to constrain the source of the observed plume. Their best fit scenario has the entire plume mass released over only a few days, from an area roughly 4.2×10^6 km^2 (80° × 15°). We assume that the release is from discrete points with an average spacing of 1, 10, or 100 km, resulting in source strengths of $Q_{1k} = 1.7 \times 10^{-5}$ kg s^{-1}, $Q_{10k} = 1.7 \times 10^{-3}$ kg s^{-1}, and Q_{100k} = 0.17 kg s^{-1}, respectively. From these modelling studies, we thus have a variety of source strengths to examine,

Table 1. Summary of Source Strengths and Diffusion-Only Results

	Strength (kg s^{-1})	CH_4 Mass (kg)	Duration (days)	18 ppbv Limits (m)	0.1 ppbv Limits (m)
Q_{60}[a]	3.66	1.86×10^7	60	1444	1493
Q_{120}[a]	1.8	1.86×10^7	120	2029	2098
Q_{344}[a]	0.63	1.86×10^7	344	3399	3517
Q_{LF}[b]	0.050	2.6×10^5	60	1404	1454
Q_{1k}[c]	1.7×10^{-5}	4.4	3	299	311
Q_{10k}[c]	1.7×10^{-3}	441	3	310	321
Q_{100k}[c]	0.17	4.4×10^4	3	320	331
Q_{Jef}	5.3×10^{-10}	1.4×10^{-4}	3	3.1 ppmv at 35 m	
Q_{COP}	1	2.6×10^5	3	3.1 ppmv at 41 m	

[a]From *Mumma et al.* [2009].
[b]From *Lefèvre and Forget* [2009].
[c]From *Mischna et al.* [2011].

extending over several orders of magnitude, summarized in Table 1.

[10] In the Jeffrey Mine, we found a source significantly weaker than those considered for Mars. To estimate its strength, we consider the diffusive mass concentration flux through the borehole, $D(\partial C/\partial z)$, and multiply it by the area through which it passes. Using a borehole diameter of 16 cm, ΔC of 200 ppmv, and Δz of 10 cm, we estimate that it is 5.3×10^{-10} kg s^{-1}. *Mumma et al.* [2009] compared their Mars observations to Coal Oil Point in Santa Barbara, which releases methane at a rate of 1.0 kg s^{-1} [*Mau et al.*, 2007], comparable to those for Mars. We evaluate our models using this strength, as well.

[11] For these source terms, the observed abundance must exceed the natural variability. At Jeffrey Mine the standard deviation of VMR_{CH_4} was 0.5 ppmv, or 32% of the background. For Mars we examine background levels of 0, 3, 6 and 10 ppbv, and examine the spatial extent of enhancements of 1, 3 and $6\sigma_{SD}$. When the background is 0 ppbv, the detection sensitivity of the MSL's Tunable Laser Spectrometer, 0.1 ppbv [*Webster and Mahaffy*, 2011], becomes the minimum VMR_{CH_4} that we are seeking. The maximum target is 28 ppbv, or six standard deviations above a background of 10 ppbv with a σ_{SD} of 3 ppb (subsequently referred to as an 18 ppbv enhancement). In general, we restrict our discussion to upper and lower limits for clarity.

5. Diffusion-Only Model With Instantaneous Release

[12] With $u = v = w = 0$ and an instantaneous source function, we consider a mass, M, of methane diffusing over time, t. The solution of the continuity equation is [*Hanna et al.*, 1982]

$$C = \frac{M}{(4\pi tD)^{3/2}} \exp\left(-\frac{x^2 + y^2 + z^2}{4tD}\right). \quad (4)$$

[13] We set $z = 1$, $y = 0$ and determine x for each concentration. Results are summarized in Table 1 for Earth and Mars.

[14] For the area source considered in *Mischna et al.* [2011], so the total mass is divided by the number of sites considered. For all three release scenarios, we found that the minimum enhancements and above were found within a distance close to 300 m from the source. For the weakest scenario, where methane sources are separated by ~1 km (total mass is 1.86×10^7 kg from 4.2×10^6 sites), we find that a VMR_{CH_4} of 0.1 ppbv is found within 311 m of one of the point sources, while an 18 ppbv enhancement occurs at 299 m. For the strongest source scenario, where sources are around 100 km apart, a VMR_{CH_4} of 0.1 ppbv is found at 331 m, and an 18 ppbv enhancement occurs at 320 m. The scenario from *Mumma et al.* [2009] uses the total mass, 1.86×10^7 kg, and longer time periods, resulting in greater spatial limits. After 60 days we find VMR_{CH_4} values of 0.1 ppbv at 1493 m and 18 ppbv at 1444 m; after 120 days 0.1 ppbv is found at 2098 m, and 18 ppbv at 2029 m; after 344 days 0.1 ppbv is found at 3517 m, and 18 ppbv at 3517 m. In the *Lefèvre and Forget* [2009] scenario, we have 2.6×10^5 kg released over 60 days and find the minimum VMR_{CH_4} 1454 m from the source while the 18 ppbv limit is only 50 m closer.

[15] Modelling the Earth scenarios this way is less informative since we are representing a continuous source with an instantaneous plume. If we consider the same short-term scenario as *Mischna et al.* [2011], 3 days, we overestimate the concentration near the source. A $6\sigma_{SD}$ VMR_{CH_4} enhancement (3.1 ppmv above background) will be seen within 34 m from the Jeffrey Mine source and 41 m from the stronger Coal Oil Point source. At Jeffrey Mine, we did not see any enhancement beyond 10 cm from the borehole, due to strong advection, and smaller released mass. We can approximate the continuous source by considering the mass released in a very small time interval, such as 1 minute, in which case the range of $6\sigma_{SD}$ VMR_{CH_4} enhancement falls to the order of 4 m.

6. Model With Mean Wind

[16] We now consider a more realistic model with wind and a continuous plume source. The average surface wind speed from the LMD-GCM is 14 ± 5 m s^{-1} at the data points around Gale Crater. We consider three wind cases, this average surface wind, light wind (5 m s^{-1}) and calm wind (0.5 m s^{-1}). The solution to the continuity equation [*Hanna et al.*, 1982] is now:

$$C = \frac{Q}{4\pi Dx} \exp\left(-\frac{y^2}{4D(x/u)} - \frac{z^2}{4D(x/u)}\right) \quad (5)$$

where x is the direction of wind with speed u, y is the distance perpendicular to the plume, z is altitude, and Q is the source strength. There are several limitations associated with this first-order model. It assumes no change in wind direction and can give the spread, in z and y, of the plume for any

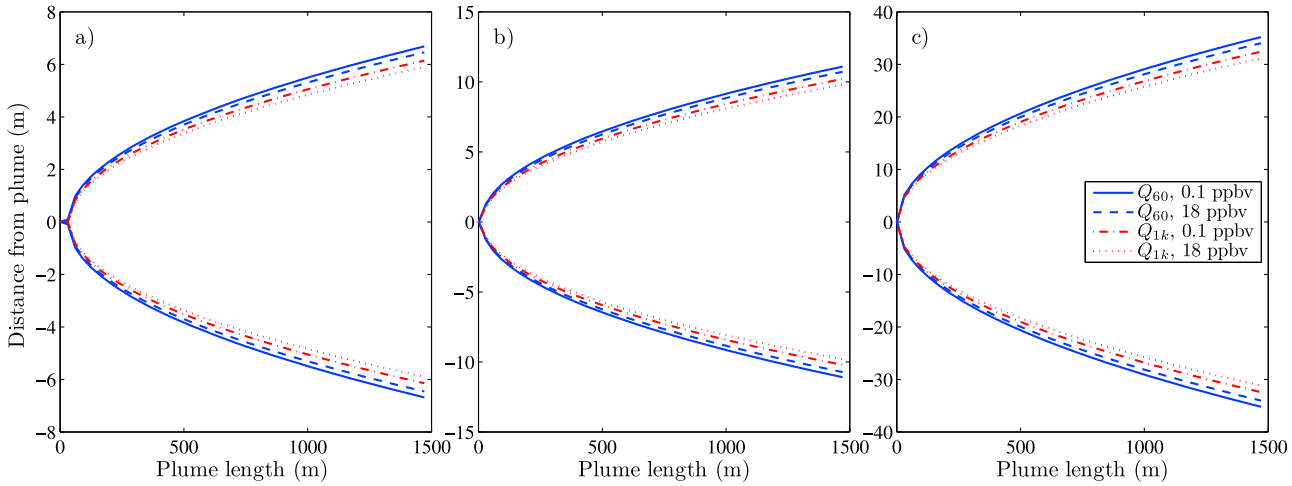

Figure 1. Model results, spatial distribution of VMR_{CH_4} at z = 1 m, for the Mars surface using a wind speed of (a) 14 m s^{-1}, (b) 5 m s^{-1}, and (c) 0.5 m s^{-1}. Two source strengths are plotted, with two detection limits each. Blue shows results for Q_{60} = 3.66 kg s^{-1}, with 0.1 ppbv (solid) and 18 ppbv (dashed) limits. Red shows results for $Q_{1k} = 1.7 \times 10^{-5}$ kg s^{-1} with 0.1 ppbv (dash-dot) and 18 ppbv (dotted) limits.

length x, which ignores large-scale advection and turbulence, therefore, it is only valid on short length scales. The assumption of constant source strength Q does not account for rapid diffusion over small time intervals, resulting in a slower decrease in concentration with y than observed on Earth. The initial conditions also assume that $C \rightarrow \infty$ as x, y, $z \rightarrow 0$ [*Hanna et al.*, 1982].

[17] This model provides a limit on the radial distance, y, along the x axis within which a methane source is larger than our imposed limit. We run the model over a 30-km downwind range to give an upper limit to diffusion-only spread and present results for the plume shape over the first 1500 m. The largest factor affecting the width of the methane plume over distance is the wind speed. Figure 1a shows the model results using the average wind speed near Gale Crater of 14 m s^{-1}. For clarity, we show only the maximum and minimum enhancement limits for the strongest source, Q_{60} = 3.66 kg s^{-1}, in blue, and the weakest source, $Q_{1k} = 1.7 \times 10^{-5}$ kg s^{-1}, in red. All cases show a maximum radial spread on the order of only ±6 m after 1.5 km, which grows to ±30 m after 30 km. The effects of reducing the wind speed to 5 m s^{-1} are shown in Figure 1b, where the width of the plume grows to ±10 m after 1.5 km, and up to ±50 m after 30 km. Calm wind conditions provide the most likely scenario for *in situ* plume detection. These are shown in Figure 1c and can have plume widths greater than ±30 m after 1.5 km. We are primarily interested in the behaviour at <100 m, since it is unlikely that the trajectory would remain stable this long.

[18] Applying the model to our two scenarios on Earth, we find that the rate of advection downwind is faster than the rate of diffusion from the plume axis. The estimated source strength in Jeffrey Mine is $Q_{Jef} = 5.3 \times 10^{-10}$ kg s^{-1}. In light wind conditions, 5 m s^{-1} the $6\sigma_{SD}$ = 3.1 ppmv limit we consider is not reached until 1.2 km downwind of the source. Calm wind conditions, 0.5 m s^{-1}, decrease the distance at which this enhancement is observed, to around 90 m. The radial range, however, is on the order of only 1–3 m. Figure 2 shows the model results for both wind conditions (in red). The stronger Coal Oil Point source (shown in blue), Q_{COP} = 1 kg s^{-1}, produces similar results, but at shorter ranges: at 60 m for calm conditions and at 800 m for light wind conditions. This source produces similar results to those found for Mars, with enhancements greater than $1\sigma_{SD}$ VMR_{CH_4} found beyond 2 m over much of the 1.5 km range shown.

7. Conclusion

[19] A simple dispersion model was applied to examine small-scale methane distributions originating from a point source on Mars and Earth. Using current estimates for Martian source strengths, we show that an *in situ* measurement that is not directly in the plume path would need to be made within 100 m of the plume axis to see appreciable

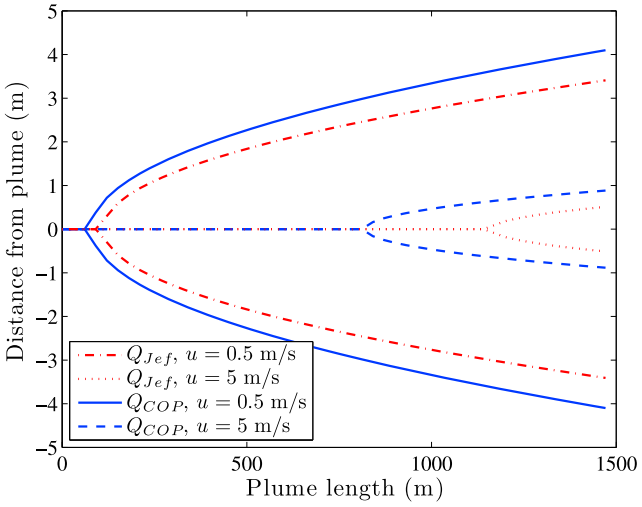

Figure 2. Model results, spatial distribution of VMR_{CH_4} at z = 1 m, for Jeffrey Mine, showing $6\sigma_{SD}$, or 3.1 ppmv, detection limits. Red shows results for $Q_{Jef} = 5.3 \times 10^{-10}$ kg s^{-1} for 5 m s^{-1} winds (dotted) and 0.5 m s^{-1} winds (dash-dot). Blue shows results for Q_{COP} = 1 kg s^{-1} for 5 m s^{-1} winds (dashed) and 0.5 m s^{-1} winds (solid).

enhancement above background levels. Our results are most strongly affected by the strength of surface winds and in light wind conditions the possibility of *in situ* measurements detecting a methane enhancement due to a local source is greatly increased. We estimated the strength of these plumes from three current modelling studies aimed at understanding recent observations [*Mumma et al.*, 2009; *Lefèvre and Forget*, 2009; *Mischna et al.*, 2011]. More recent observations have been published [*Fonti and Marzo*, 2010; *Geminale et al.*, 2011; *Krasnopolsky*, 2012] and current modelling work will continue to focus on determining the optimal methane source conditions. A new set of highly sensitive *in situ* measurements will also be made within the year by the Mars Science Laboratory, which will provide the best constraints on the background methane concentration to date.

[20] This work was motivated by finding weak methane sources at Jeffrey Mine and determining that it is unlikely that a deployed micro-rover could detect an enhancement autonomously. Since these measurements were made as part of a Mars analogue mission, we wanted to place these findings in the context of the Mars surface environment. We estimated a source strength of 5.3×10^{-10} kg s^{-1} at Jeffrey Mine and found that this weak a source cannot produce measurable enhancements of 0.5 to 3.1 ppmv above background levels (1.6 ppmv) within reasonable length scales when wind is present. Under calm wind conditions (0.5 m s^{-1}), the plume would have to travel over 90 m before the plume broadens from its axis enough to produce a $6\sigma_{SD}$ = 3.1 ppmv enhancement, and then a measurement would need to be made within meters of the plume axis, so the chance of identifying it remains dubious.

[21] **Acknowledgments.** The M3 analogue mission to Jeffrey Mine was funded by the Canadian Space Agency (CSA) and operated through MPB Communications. M3 is a collaboration between MPB, the University of Winnipeg, McGill University, Carleton University, the University of Toronto, and the Université du Québec à Montréal. The Kapvik micro-rover is being developed jointly by MPB and Carleton University. We thank Lyle Whyte, Diana Popa and Roland Wilhel for providing the Picarro data and everyone who participated in the first M3 field deployment in 2011. We also thank the LMD-GCM team for making their model accessible for researchers.

[22] The Editor thanks two anonymous reviewers for their assistance in evaluating this paper.

References

Catalfamo, C., D. Bruno, G. Colonna, A. Laricchiuta, and M. Capitelli (2009), High temperature Mars atmosphere. Part II: Transport properties, *Eur. Phys. J. D*, *54*, 613–621, doi:10.1140/epjd/e2009-00193-6.

Chapman, S., and T. Cowling (1970), *The Mathematical Theory of Non-uniform Gases*, Cambridge Univ. Press, New York.

Cloutis, E. A., et al. (2012), The Mars Methane Analogue Mission (M3): Results of the 2011 field deployment, in *Proc. Lunar Planet. Sci. Conf.*, *43*, Abstract 1569, Lunar and Planetary Institute, Houston, Tx.

Cowie, M., and H. Watts (1971), Diffusion of methane and chloromethanes in air, *Can. J. Chem.*, *49*, 74–77.

Fonti, S., and G. A. Marzo (2010), Mapping the methane on Mars, *Astron. Astrophys.*, *512*, A51, doi:10.1051/0004-6361/200913178.

Forget, F., F. Hourdin, R. Fournier, C. Hourdin, O. Talagrand, M. Collins, S. R. Lewis, P. L. Read, and J.-P. Huot (1999), Improved general circulation models of the Martian atmosphere from the surface to above 80 km, *J. Geophys. Res.*, *104*, 24,155–24,176, doi:10.1029/1999JE001025.

Formisano, V., S. Atreya, T. Encrenaz, N. Ignatiev, and M. Giuranna (2004), Detection of methane in the atmosphere of Mars, *Science*, *306*, 1758–1761, doi:10.1126/science.1101732.

Geminale, A., V. Formisano, and G. Sindoni (2011), Mapping methane in Martian atmosphere with PFS-MEX data, *Planet. Space Sci.*, *59*, 137–148, doi:0.1016/j.pss.2010.07.011.

Gough, R. V., M. A. Tolbert, C. P. McKay, and O. B. Toon (2010), Methane adsorption on a Martian soil analog: An abiogenic explanation for methane variability in the Martian atmosphere, *Icarus*, *207*, 165–174, doi:10.1016/j.icarus.2009.11.030.

Hanna, S. R., G. A. Briggs, and R. P. Hosker Jr. (1982), *Handbook on Atmospheric Diffusion, Tech. Rep. DOE/TIC-11223*, Tech. Inf. Cent., U.S. Dep. of Energy, Springfield, Va.

Hudson, T. L., and O. Aharonson (2008), Diffusion barriers at Mars surface conditions: Salt crusts, particle size mixtures, and dust, *J. Geophys. Res.*, *113*, E09008, doi:10.1029/2007JE003026.

Hudson, T. L., O. Aharonson, N. Schorghofer, C. B. Farmer, M. H. Hecht, and N. T. Bridges (2007), Water vapor diffusion in Mars subsurface environments, *J. Geophys. Res.*, *112*, E05016, doi:10.1029/2006JE002815.

Izakov, M. N. (1978), The Martian upper atmosphere structure from the Viking spacecraft experiments, *Icarus*, *36*, 189–197, doi:10.1016/0019-1035(78)90103-3.

Krasnopolsky, V. A. (2012), Search for methane and upper limits to ethane and SO_2 on Mars, *Icarus*, *217*, 144–152, doi:10.1016/j.icarus.2011.10.019.

Krasnopolsky, V. A., J. P. Maillard, and T. C. Owen (2004), Detection of methane in the Martian atmosphere: Evidence for life?, *Icarus*, *172*, 537–547, doi:10.1016/j.icarus.2004.07.004.

Laurent, A., and Y. Hébert (1979), Paragenesis of serpentine assemblages in harzburgite tectonite and dunite cumulate from the Québec Appalachians, *Can. Mineral.*, *17*, 857–869.

Lefèvre, F., and F. Forget (2009), Observed variations of methane on Mars unexplained by known atmospheric chemistry and physics, *Nature*, *460*, 720–723, doi:10.1038/nature08228.

Lindal, G. F., H. B. Hotz, D. N. Sweetnam, Z. Shippony, J. P. Brenkle, G. V. Hartsell, and R. T. Spear (1979), Viking radio occultation measurements of the atmosphere and topography of Mars: Data acquired during 1 Martian year of tracking, *J. Geophys. Res.*, *84*, 8443–8456, doi:10.1029/JB084iB14p08443.

Mau, S., D. L. Valentine, J. F. Clark, J. Reed, R. Camilli, and L. Washburn (2007), Dissolved methane distributions and air-sea flux in the plume of a massive seep field, Coal Oil Point, California, *Geophys. Res. Lett.*, *34*, L22603, doi:10.1029/2007GL031344.

Mischna, M. A., M. Allen, M. I. Richardson, C. E. Newman, and A. D. Toigo (2011), Atmospheric modeling of Mars methane surface releases, *Planet. Space Sci.*, *59*, 227–237, doi:10.1016/j.pss.2010.07.005.

Mumma, M. J., R. E. Novak, M. A. DiSanti, B. P. Bonev, and N. Dello Russo (2004), Detection and mapping of methane and water on Mars, *Bull. Am. Astron. Soc.*, *36*, 1127.

Mumma, M. J., G. L. Villanueva, R. E. Novak, T. Hewagama, B. P. Bonev, M. A. DiSanti, A. M. Mandell, and M. D. Smith (2009), Strong release of methane on Mars in northern summer 2003, *Science*, *323*, 1041–1045, doi:10.1126/science.1165243.

Owen, T., K. Biemann, J. E. Biller, A. L. Lafleur, D. R. Rushneck, and D. W. Howarth (1977), The composition of the atmosphere at the surface of Mars, *J. Geophys. Res.*, *82*, 4635–4639, doi:10.1029/JS082i028p04635.

Pinet, N., and A. Tremblay (1995), Tectonic evolution of the Quebec-Maine Appalachians; from oceanic spreading to obduction and collision in the northern Appalachians, *Am. J. Sci.*, *295*, 173–200, doi:10.2475/ajs.295.2.173.

Reid, R. C., J. M. Prausnitz, and B. E. Poling (1987), *The Properties of Liquids and Gases*, 4th ed., McGraw-Hill, New York.

Richardson, M. I., A. D. Toigo, and C. E. Newman (2007), PlanetWRF: A general purpose, local to global numerical model for planetary atmospheric and climate dynamics, *J. Geophys. Res.*, *112*, E09001, doi:10.1029/2006JE002825.

Rodrigo, R., E. Garcia-Alvarez, M. J. Lopez-Gonzales, and M. A. Lopez-Valerde (1990), Estimates of eddy diffusion coefficient in the Mars' atmosphere, *Atmosfera*, *3*, 31–43.

Smith, D., G. Neumann, P. Ford, R. E. Arvidson, E. A. Guinness, and S. Slavney (1999), Mars Global Surveyor Laser Altimeter Precision Experiment data record, *Tech. Rep. MGS-M-MOLA-3-PEDR-L1A-V1.0*, NASA Planet. Data Syst., College Park, Md.

Webster, C. R., and P. R. Mahaffy (2011), Determining the local abundance of Martian methane and its $^{13}C/^{12}C$ and D/H isotopic ratios for comparison with related gas and soil analysis on the 2011 Mars Science Laboratory (MSL) mission, *Planet. Space Sci.*, *59*, 271–283, doi:10.1016/j.pss.2010.08.021.

Wong, A.-S., S. K. Atreya, and T. Encrenaz (2003), Chemical markers of possible hot spots on Mars, *J. Geophys. Res.*, *108*(E4), 5026, doi:10.1029/2002JE002003.

Zahnle, K., R. S. Freedman, and D. C. Catling (2011), Is there methane on Mars?, *Icarus*, *212*, 493–503, doi:10.1016/j.icarus.2010.11.027.